

Adv. Polar Upper Atmos. Res., **15**, 1–10, 2001

## Electric fields and meteor radar wind measurements near 95 km over South Pole

J.M. Forbes<sup>1</sup>, M.J. Jarvis<sup>2</sup>, S.E. Palo<sup>1</sup>, X. Zhang<sup>1</sup>,  
Yu.I. Portnyagin<sup>3</sup> and N.A. Makarov<sup>3</sup>

<sup>1</sup> *Department of Aerospace Engineering Sciences, UCB 429, University of Colorado, Boulder, CO 80309-0429, U.S.A.*

<sup>2</sup> *British Antarctic Survey, Madingley Road, Cambridge CB3 0ET, United Kingdom*

<sup>3</sup> *Institute for Experimental Meteorology, Lenin Str. 82, Obninsk, Kaluga Region, 249020, Russia*

**Abstract:** Meteor and auroral drift measurements by P. Prikryl *et al.* (Radio Sci., **21**, 271, 1986) and theoretical estimates by G.C. Reid (Radio Sci., **18**, 1028, 1983) suggest that sufficiently large electric fields may decouple meteor trail electron motions from that of the neutral gas, leading to erroneous measurement of the neutral wind during sufficiently disturbed conditions. In the present study, we seek evidence of such effects by comparing hourly meteor radar wind measurements  $V_N$  near 95 km over South Pole with overhead *F*-region drifts  $V_i$  measured by the SuperDARN radar at Halley (76°S, 27°W). Within the parameter space of our data set, we find no relationship between  $V_i$  and the zonal wavenumber  $s=0$  and  $s=1$  components of  $V_N$ , and only a weak relationship for the wind residuals from the combined  $s=0$  and  $s=1$  wind field. For the latter, an inferred wind residual of  $5.8 \text{ ms}^{-1}$  is implied for an *F*-region plasma drift of  $1000 \text{ ms}^{-1}$  ( $E$ -field  $\approx 70 \text{ mVm}^{-1}$ ). This value of  $5.8 \text{ ms}^{-1}$  falls within the 2 to  $20 \text{ ms}^{-1}$  range of plasma drifts expected to be induced at 95 km by *F*-region  $E$ -fields ranging between 20 and  $100 \text{ mVm}^{-1}$  by G.C. Reid (*ibid.*, 1983). Thus, we cannot discount the possibility that this inferred wind is actually a plasma drift. In any case, we conclude that electric field contamination of previous scientific analyses with this data set which focused on the  $s=0$  and  $s=1$  components of the wind field, are negligible. Future experimental and modeling work is required to ascertain the degree to which  $E$ -field induced effects on winds inferred from advection of meteor trails exist under more extreme conditions, or perhaps over shorter time scales.

### 1. Introduction

A meteor radar was operated at Amundsen-Scott Station, South Pole, from January 19, 1995 through January 26, 1996 and from November 21, 1996 through January 27, 1997. Hourly wind measurements were obtained nearly continuously over these time periods, at an approximate altitude of 95 km and at about 2° latitude from South Pole along the geographic longitude meridians 0°, 90°E, 90°W, and 180°. A number of scientific advances emerged from analyses of the wind data (Forbes *et al.*, 1995, 1999a, b; Palo *et al.*, 1998; Portnyagin *et al.*, 1997, 1998, 2000). These include: (1) Strong divergences of zonal-mean meridional winds occasionally occur over South Pole, implying extreme vertical winds; (2) The monthly mean zonally asymmetric (zonal

wavenumber  $s = 1$ ) wind component varies during the year in a manner consistent with migration of the center of the polar vortex with respect to the geographic (rotational) pole; (3) Strong ( $> 15$  m/s) westward-propagating migrating trapped diurnal and non-migrating semidiurnal oscillations exist except during winter months; (4) Long-period ( $\sim 2$ – $10$  days) waves exist during winter months which are primarily eastward-propagating; (5) Intradiurnal (periods  $\sim 6$ – $11.5$  hours) westward-propagating oscillations exist, which are thought to be gravitational normal modes, or “Lamb” waves. All of the aforementioned zonally propagating oscillations are characterized by zonal wavenumber  $s = 1$  in the meridional wind field.

The meteor radar method for measuring winds assumes that collision frequencies are sufficiently large that the ionized meteor trails assume a bulk motion equal to that of the ambient neutral wind. Combined meteor and auroral drift measurements by Prikryl *et al.* (1986) and theoretical estimates by Reid (1983) suggest that sufficiently large electric fields may decouple meteor trail electron motions from that of the neutral gas, leading to erroneous measurement of the neutral wind during sufficiently disturbed conditions. Balsley *et al.* (1982) note a relationship between inferred neutral winds at Poker Flat and auroral electrojet fluctuations which may also represent some influence of electric fields on meteor trails. Herein we attempt to ascertain the importance of this effect specifically for the neutral winds inferred from the South Pole meteor radar measurements. This is accomplished through a comparative analysis between  $F$ -region drifts (equivalently,  $E$ -fields which map down to the lower  $E$ -region with some attenuation and rotation) measured over the South Pole region by the SuperDARN radar at Halley ( $76^\circ$  S,  $27^\circ$  W), Antarctica, and neutral winds measured by meteor radar near 95 km from South Pole. These experiments are briefly described in the following.

## 2. Halley Bay SuperDARN plasma drift measurements

The HF radar (Greenwald *et al.*, 1985) at Halley ( $76^\circ$  S,  $27^\circ$  W), Antarctica, which has operated since 1988, is part of the Super Dual Auroral Radar Network (SuperDARN) (Greenwald *et al.*, 1995). This over-the-horizon radar operates on a fixed frequency, normally between 12 MHz and 14 MHz and with its 16 beams it provides an azimuth scan of 52 degrees every 2 min. It typically samples in 45-km deep range bins covering ranges from 270 km out to 3420 km, and its field-of-view consequently includes South Pole ( $90^\circ$  S). The radar is sensitive to decametric ionospheric irregularities and measures the power and line-of-sight Doppler spectral characteristics of the signal returns from them. In the ionospheric  $F$ -region these irregularities move with the background plasma flow (Ruohoniemi *et al.*, 1987) and thus reveal the plasma drift vector  $\vec{E} \times \vec{B} / B^2$  and thereby the electric field.

The field of view of the Halley drift measurements in relation to the South Pole wind measurements in geographic and invariant magnetic coordinate systems is illustrated in Fig. 1. An example of the plasma drift measurements over the span of one hour Universal Time is provided in Fig. 2. The components are calculated parallel and perpendicular to a given  $L$  shell, and are assumed constant over the longitude range of the beam. Note that the geographic coordinates (latitude =  $88^\circ$ ; longitudes =  $0^\circ$ ,  $90^\circ$ ,  $180^\circ$ ,  $270^\circ$  E) of the neutral wind measurements lie between invariant latitudes

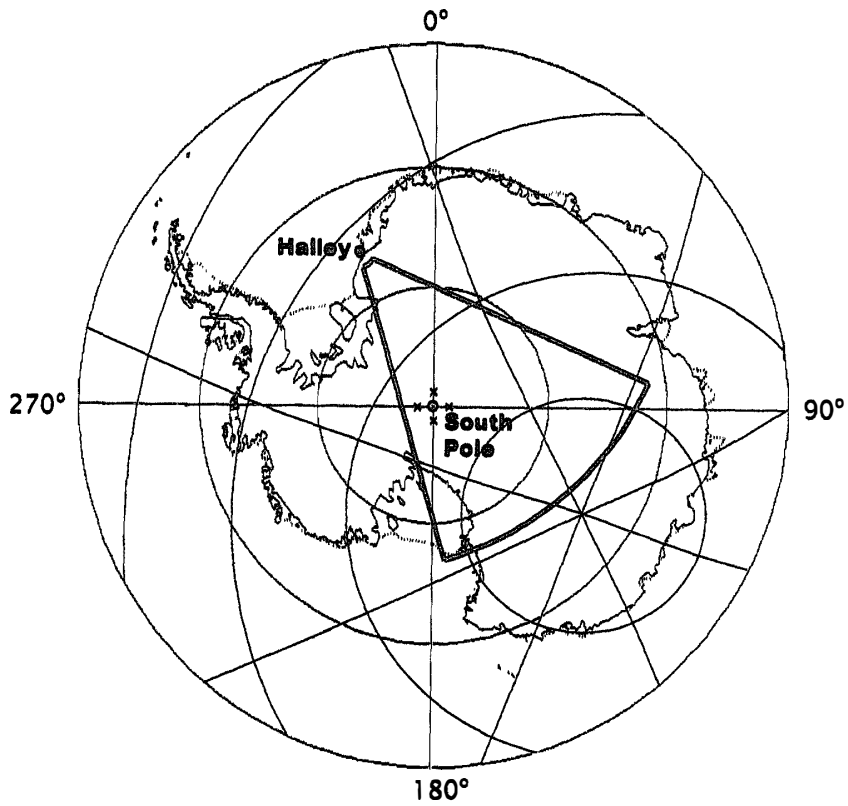


Fig. 1. Field of view of SuperDARN plasma drift measurements from Halley (green) and locations of South Pole meridional wind measurements at 95 km (crosses) in geographic (solid black) and invariant magnetic (light blue) coordinates.

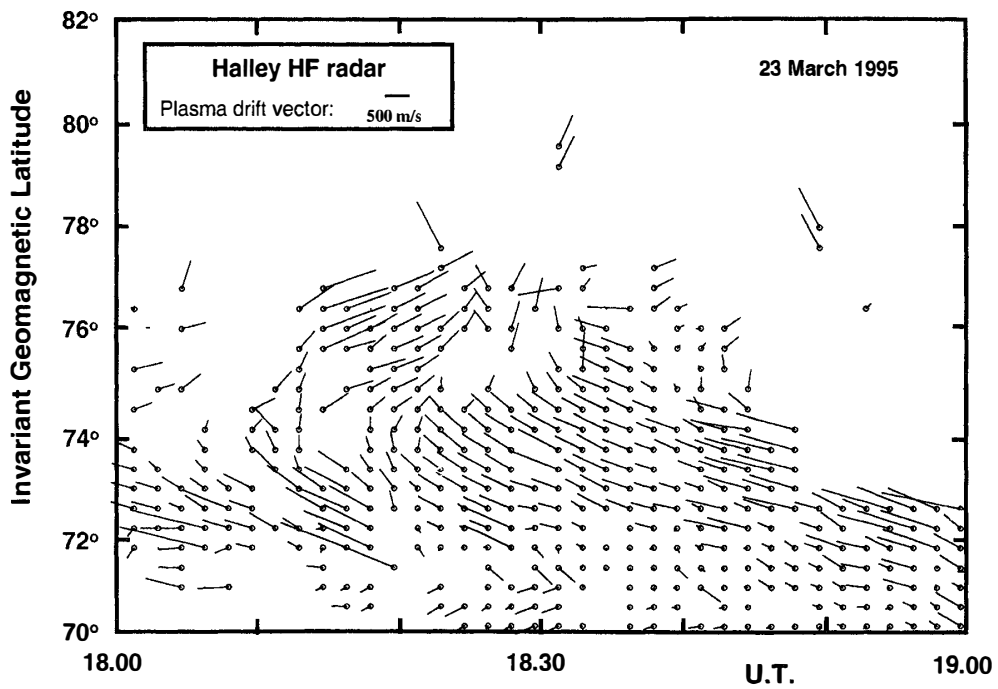


Fig. 2. Sample of 1 hour's measurements of plasma drifts from the SuperDARN radar at Halley plotted vs. invariant latitude and Universal Time for March 23, 1995.

$\Lambda = 70^\circ - 79^\circ$  and invariant longitudes  $0^\circ - 30^\circ$ .

### 3. South Pole meteor radar wind measurements

Portnyagin *et al.* (1997, 1998) and Palo *et al.* (1998) describe the meteor radar system and various error estimates. An abbreviated description is provided here. In the meteor radar technique, winds are detected by measuring the Doppler shift of coherent radio reflections from the ionized trails produced by meteor ablation in the upper atmosphere. The meteor trails are several kilometers in length, with an initial radius of about 1 meter. The South Pole system operates at a frequency of 33.57 MHz, with a peak power of 7 kW, a pulse width of 120 microseconds and a pulse repetition frequency of either 100 or 300 Hz (see below). The radar operates in a monostatic configuration with four five-element Yagi transmitting/receiving antennae, directed in the horizontal plane along the  $0^\circ$ ,  $90^\circ$  E,  $180^\circ$ , and  $90^\circ$  W geographical meridians. In the vertical plane the antennae are directed at an elevation angle of  $28^\circ$ . The two-way halfpower-halfwidths of the antenna beams are about  $20^\circ$  in both azimuth and elevation, which translate to minor uncertainties in our wind estimates (Palo *et al.*, 1998). The hourly mean winds, which are assumed to be horizontal, represent Gaussian-weighted averages centered near 95 km above sea level. As a result, the system is only sensitive to wave structures with vertical wavelengths exceeding about 20 km (Palo *et al.*, 1998). (N.B.: The only wind component measured from South Pole is the meridional wind, taken here to be positive in the southward direction).

The system operates in two modes. In the search mode, the atmosphere is “interrogated” with frequency 100 Hz for the appearance of reflections from meteor trails. When a meteor echo is detected in any direction, the search mode is stopped and pulses with repetition frequency of 300 Hz are radiated. A number of measures exist to ensure that “good” echoes, *i.e.*, those that lead to reliable Doppler shifts (wind measurements), are selected while others are rejected. In particular, the interrogation/acquisition sequence automatically eliminates a number of spurious and unreliable echoes from the analysis. Auroral echoes have a number of characteristic features that allow them to be identified and then rejected. About 5000 valid meteor echoes are acquired per day.

### 4. Methodology and results

Our methodology for evaluating possible *E*-field contamination of neutral winds inferred from meteor trail advection consists of establishing the existence of common variations between the plasma drifts measured by SuperDARN and the neutral winds measured from South Pole. There are a number of limitations and caveats associated with this approach. First, the above criterion is a necessary but not sufficient condition for electric-field induced motions, since neutral winds may exist that have their driving force in electrodynamic origins (*i.e.*, Balsley *et al.*, 1982; Prikryl *et al.*, 1986). Second, since the SuperDARN measurements are not nearly as continuous as the meteor radar measurements, it is necessary to establish this relationship *statistically* over the whole data set, rather than to study a number of disturbance “events” wherein sudden

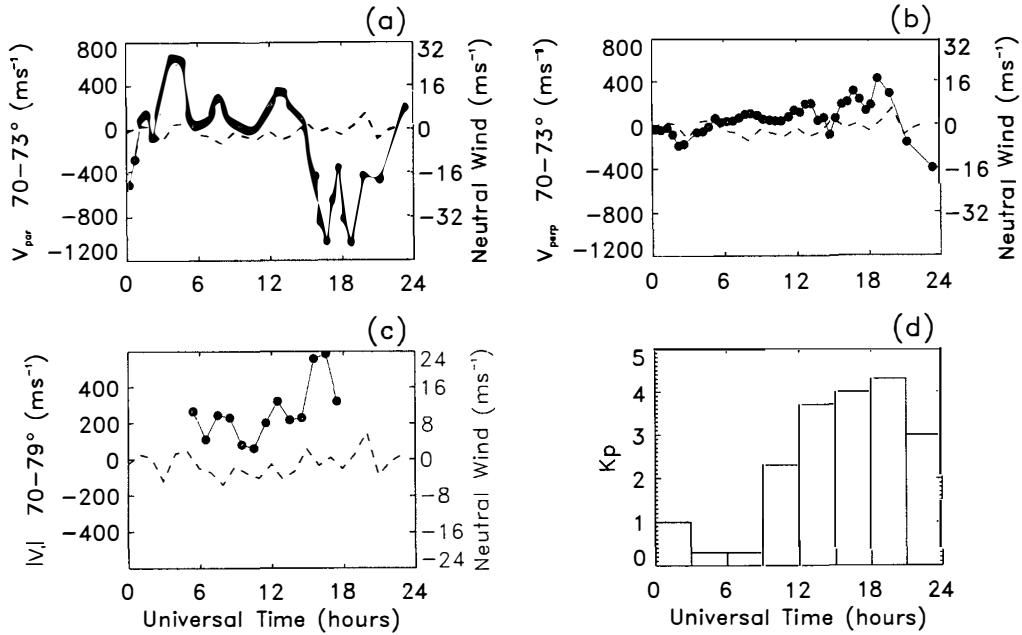


Fig. 3. Comparisons between several plasma drift parameters (solid dots/lines) and the neutral wind residual (dashed lines)  $V_{RI}$  in the  $0^\circ$  longitude direction on April 22, 1995, when SuperDARN measurements were nearly continuous and magnetic activity levels increased from very quiet to moderately disturbed. (a) Component of plasma drift vector  $\vec{V}_i$  parallel to L-shell (eastward) averaged over  $70-73^\circ$  invariant magnetic latitude ( $\Lambda$ ); (b) component of plasma drift vector  $\vec{V}_i$  perpendicular to L-shell (poleward) averaged over  $\Lambda = 70-73^\circ$ ; (c) amplitude of plasma drift vector  $|\vec{V}_i|$  averaged over  $\Lambda = 70-79^\circ$ ; and (d) planetary geomagnetic index  $K_p$  during April 22, 1995.

increases in the electric field might suggest some cause-effect relationship with the neutral winds. A typical example of one of only a few such disturbance events when near-continuous plasma drift measurements were available is provided in Fig. 3 (a-d). On this day, April 22, 1995,  $K_p$  increased from very quiet to moderately disturbed levels ( $4^0-4^+$ ) over about 9 hours. While excursions in the plasma drift components were of order  $500-1000 \text{ ms}^{-1}$ , no perceptible change in the residual neutral wind (defined below) in the  $0^\circ$ -longitude direction occurred in concert with the changes in plasma drift. However, confining ourselves to a few disturbance events eliminates many coincident neutral wind/plasma drift measurements from consideration. Therefore a search for a statistical relationship is pursued below. Moreover, by limiting our consideration to hourly values in the present study, we furthermore do not preclude the possible existence of electric-field-induced motion of the meteor trails over shorter time scales. Nevertheless, despite the above limitations, we have been able to obtain some useful results relevant to our stated goal of establishing the efficacy of the hourly wind measurements and scientific results that have been published from this meteor radar wind data set.

In pursuing the possible existence of a statistical relationship between plasma drifts and neutral winds, we examined the correlations between several parameters relating to both data fields. For the plasma drifts, we considered the eastward and southward components in invariant magnetic coordinates; the amplitude of the total drift vector; values calculated separately for the invariant latitude bins  $\Lambda = 70-73^\circ$ ,  $73-76^\circ$ ,  $76-79^\circ$

as well as values averaged over the whole latitude range  $70\text{--}79^\circ$ . For the neutral winds, we considered the components in the four azimuth directions as well as the total wind vector over the pole; residual wind values from fits which included the diurnal and semidiurnal tides; and residual values from hourly fits which included zonal wavenumber  $s=1$ . In virtually all cases, no perceptible correlation was found whatsoever. Below, we report on the one single combination of drift and neutral wind parameters that yield the slightest hint of a relationship.

As noted in the Introduction, a significant portion of the wind field over South Pole is characterized by eastward and westward propagating waves with zonal wavenumber  $s=1$ , and periods ranging from 7 hours to several days. There is no reason to expect that E-field or any geomagnetically related effects would be manifested in the form of  $s=1$  zonal structures around the *geographic* pole (refer to Fig. 1). (This will be verified later.) Therefore, for each hour's measurements, the neutral wind observations in the four azimuth directions were least-squares fit with a function of the form

$$V = V_0 + A \cos\lambda + B \sin\lambda, \quad (1)$$

where  $V_0$ ,  $A$  and  $B$  are constants,  $\lambda$  is longitude, and a set of wind residuals are formed by subtracting (1) from each hourly measurement in each azimuth direction. Later, we will utilize the amplitude of the  $s=1$  wind component,  $A_1 = \sqrt{A^2 + B^2}$ , in our discussions. If we define  $r_1$ ,  $r_2$ ,  $r_3$ , and  $r_4$  to denote these residuals in the respective azimuth (longitude) directions  $0^\circ$ ,  $90^\circ$ ,  $180^\circ$ ,  $270^\circ$ , then it may be shown that the residuals must conform to the following relationships if the fit is to be optimized in a least-squares sense:

$$r_1 = r_3; r_2 = r_4; r_1 = -r_2. \quad (2)$$

Typical examples of the fit of eq. (1) to raw South Pole wind measurements, illustrating the  $r_1$ ,  $r_2$ ,  $r_3$ , and  $r_4$  wind residuals, are provided in Fig. 4. Therefore, it is only necessary to analyze one of these residuals, which we choose to be  $r_1$ , hereafter-denoted  $V_{R1}$ . The above residual values, which are generally less than  $10 \text{ ms}^{-1}$ , represent that part of the measured wind field over the geographic South Pole which does not conform to an  $s=1$  zonal structure, and which therefore might bear some relation to electric field variations. The plasma drift parameter that correlated best with  $V_{R1}$  is the hourly mean amplitude of the drift vector averaged over  $70\text{--}79^\circ$  latitude, hereafter denoted  $|\bar{V}_i|$ . Recall from previous discussion that the plasma drift vector is assumed to be constant over the  $0\text{--}30^\circ$  range of invariant longitudes.

Scatter plots comparing  $V_0$ ,  $A_1$ , and  $V_{R1}$  as defined in connection with eq. (1), vs. all available values of  $|\bar{V}_i|$ , are illustrated in Fig. 5. A Linear least-square fits, to a simple model  $= m |\bar{V}_i| + b$ , and the corresponding correlation coefficients  $R$  are also illustrated. Table 1 summarizes these results that include computation of the correlation coefficient, Spearman rank correlation coefficient (Mendenhall *et al.*, 1986), a linear least squares fit and statistical significance levels. The results of a two-sided hypothesis test favor the null hypothesis, that there is no correlation between variables, for the mean and zonal wavenumber 1 component ( $V_0$ ,  $A_1$ ). Conversely the alternative hypothesis, indicating a non-zero correlation, is favored in the case of the residual ( $V_{R1}$ ). Both the Spearman rank correlation and least-squares fit indicate a statistically significant correlation

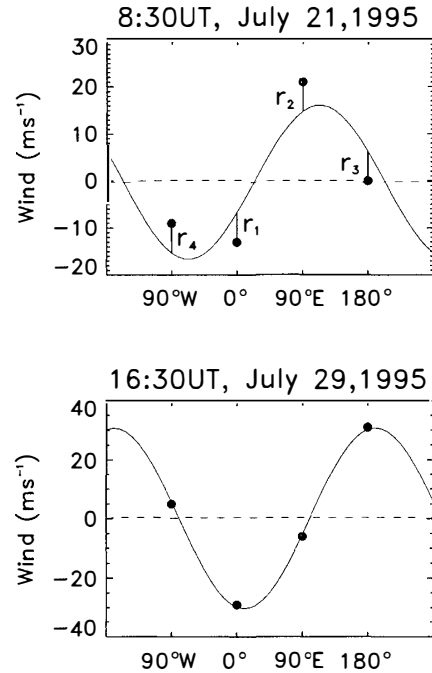


Fig. 4. Sample fits of raw South Pole wind measurements with a zonal wavenumber  $s=1$  structure, illustrating the  $r_1$ ,  $r_2$ ,  $r_3$  and  $r_4$  wind residuals.

between  $|\bar{V}_i|$  and  $V_{r1}$ , albeit this correlation is rather weak ( $R=0.23$ ). The results of the least squares fits through the wind residuals suggest a possible effect of  $\sim 5.8 \text{ ms}^{-1}$  for a plasma drift of  $1000 \text{ ms}^{-1}$ , which corresponds roughly to an electric field magnitude of  $70 \text{ mVm}^{-1}$ . However, it is important to note that the correlation coefficient for this fit is only  $R=0.23$ , implying that  $R^2 \approx 0.04$ , and hence only about 4% of the variability of  $V_{r1}$  is accounted for by this linear relationship with  $|\bar{V}_i|$ .

The above results for  $V_0$  are consistent with the finding of Portnyagin *et al.* (1997) that geomagnetic effects are negligible based on the lack of correlation between the zonally-averaged wind field and the global geomagnetic index,  $K_p$ . Similar conclusions are drawn here for the  $s=1$  component of the wind field, confirming intuitive expectations (*i.e.*, there is no reason to expect any relation between neutral wind structures which conform to a  $s=1$  zonal structure around the *geographic* pole with electrodynamic effects ordered in geomagnetic coordinates).

Results for  $V_{R1}$  in the lower panel of Fig. 5, while weak, are now interpreted in light of the estimates of Reid (1983). Reid has estimated the contaminating effects of electric fields on the inference of neutral winds from the motion of weak spherical plasma irregularities in the region between 60 and 120 km. Estimates for the more intense cylindrical meteor trail columns are expected to be similar, unless closely aligned with the magnetic field (Reid, 1983). According to Reid, irregularity drift velocities at 95 km range from about 2 to  $20 \text{ ms}^{-1}$  for “average” to “very disturbed” magnetic conditions, *i.e.*, assuming magnetospheric electric fields of order 20 to  $100 \text{ mVm}^{-1}$  and allowing a factor of two attenuation down to the region of interest. Our estimate of a possible effect of order  $5 \text{ ms}^{-1}$  for an  $F$ -region field of  $70 \text{ mVm}^{-1}$  falls within this range. However, from our data we cannot determine to what extent the  $5 \text{ ms}^{-1}$  inferred wind is truly a neutral atmosphere response to disturbed geomagnetic conditions or is a non-neutral drift induced by the presence of a strong geomagnetic field. The separation

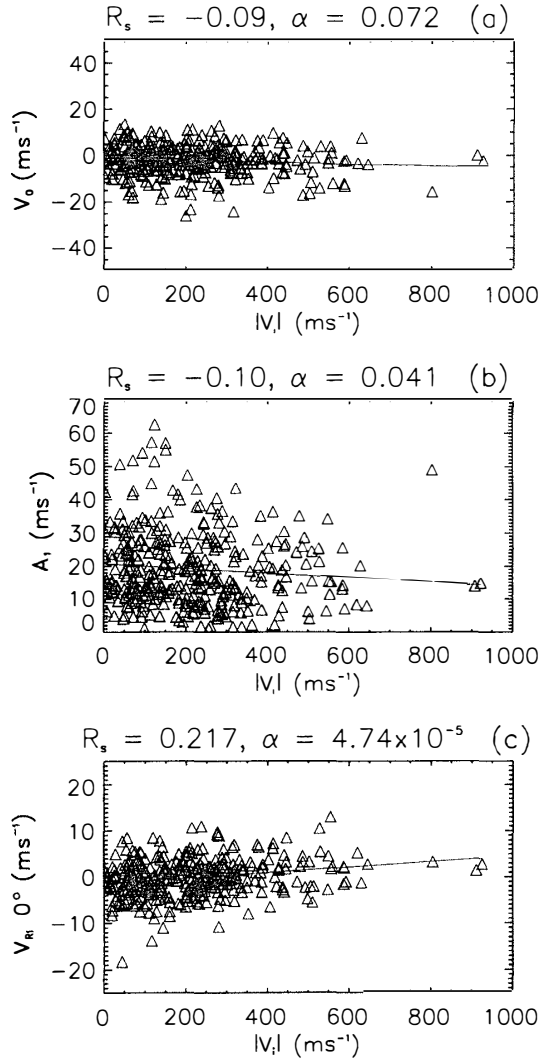


Fig. 5. Scatter plots of  $V_0$  (top),  $A_1$  (middle) and  $V_{R1}$  (bottom) as defined in connection with eq. (1) in the text, vs. the hourly magnitude of the plasma drift vector  $|\bar{V}_i|$  averaged over  $70^\circ$ – $79^\circ$  invariant magnetic latitude. The Spearman rank correlation value ( $R_s$ ) and type I error ( $\alpha$ ) are indicated for each plot.

Table 1. Correlation coefficients and statistical significance for three cases ( $V_0$ ,  $A_1$  and  $V_{R1}$ ) are shown. Illustrated are the correlation coefficient ( $R$ ), Spearman rank correlation coefficient ( $R_s$ ), type I error for a two-sided hypothesis test ( $\alpha$ ), statistical significance level ( $(1-\alpha) \times 100\%$ ), slope from a linear least squares fit ( $m$ ) and the  $1-\alpha$  confidence interval for the fitted parameter.

Case	$R$	$R_s$	$\alpha$	$(1-\alpha) \times 100\%$	$m$	$\sigma_m$	Significance
$V_0$	-0.101	-0.0968	0.0728	92.7%	-0.0046	0.0025	None
$A_1$	-0.0997	-0.1099	0.0417	95.8%	-0.0072	0.0039	Marginal
$V_{R1}$	+0.226	+0.217	0.000047	99.99%	+0.0058	0.0013	High

of these two effects requires the careful design of an experiment with measurements from collocated meteor and incoherent scatter radars in addition to a sodium lidar.

## 5. Conclusions

From this study we conclude that electric field contamination of the  $s=0$  and



$s=1$  components of the neutral wind field derived from hourly meteor radar data over the South Pole are negligible. Thus, the efficacy of previous analyses conducted with this data set are confirmed. Some evidence exists for enhanced neutral wind residuals from the  $s=0$  and  $s=1$  structures, of order  $5 \text{ ms}^{-1}$  for an  $F$ -region field of  $70 \text{ mVm}^{-1}$ , which is consistent with estimates by Reid (1983) for electric-field-induced drift of the meteor trail. However, from our measurements, it is not possible to discern whether the meteor trail drift is due to a neutral wind or an electric field.

However, it is important to understand that our conclusions only apply to the parameter space of our data set and should not be extrapolated to other conditions. Factors related to our method of deriving neutral winds that may ameliorate the effects of electric fields include 1-hour averaging and rejection of aurorally contaminated echoes. As noted by Reid (1983), fields of large horizontal scale are expected to map down with little attenuation compared to smaller-scale fields which intuitively would also be characterized by shorter time scales. In our method of analysis, which involves averaging over space and time to arrive at an estimate of the  $F$ -region electric field, we may have extracted that component which preferentially maps down to 95 km and is thus able to influence the motion of meteor trails. In addition, larger electric fields may be experienced at latitudes where auroral conditions are more prevalent than at South Pole. It should be emphasized that Reid (1983) studied the weak, small-scale irregularities in refractive index observed by MST radars. As noted by Reid (1983), results for the very different geometry and high line density of ionization in a meteor trail will not be the same as a volume distribution of weak ionization.

Much remains to be done concerning the effects of electric fields on the inference of neutral winds from the motions of meteor trails, especially at time scales shorter than 1 hour or under more intense electric field conditions. The ideal experiment for this purpose would be measurements from co-located meteor and incoherent scatter radars at an auroral location (*i.e.*, Sondrestrom or EISCAT).

### Acknowledgments

This work was supported by Grant ATM-9728993 from the National Science Foundation to the University of Colorado.

The editor thanks Dr. G. Fraser and another referee for their help in evaluating this paper.

### References

- Balsley, B.B., Carter, D.A. and Eucklund, W.L. (1982): On the relationship between auroral electrojet fluctuations and the wind field near the mesopause. *Geophys. Res. Lett.*, **9**, 219.
- Forbes, J. M., Makarov, N.A. and Portnyagin, Yu.I. (1995): First results from the meteor radar at South Pole: A large 12-hour oscillation with zonal wavenumber one. *Geophys. Res. Lett.*, **22**, 3247–3250.
- Forbes, J.M., Portnyagin, Yu.I., Makarov, N.A., Palo, S.E., Merzlyakov, E.G. and Zhang, X. (1999a): Dynamics of the lower thermosphere over South Pole from meteor radar wind measurements. *Earth Planets Space*, **51**, 611–620.
- Forbes, J.M., Palo, S.E., Zhang, X., Portnyagin, Yu.I., Makarov, N.A. and Merzlyakov, E.G. (1999b): Lamb waves in the lower thermosphere: Observational evidence and global consequences. *J. Geophys. Res.*, **104**, 17107–17114.

- Greenwald, R. A., Baker, K. B., Hutchins, R. A. and Hanuise, C. (1985): An HF phased-array radar for studying small-scale structure in the high-latitude ionosphere. *Radio Sci.*, **20**, 63–79.
- Greenwald, R.A., Baker, K.B., Dudeney, J.R., Pinnock, M., Jones, T.B., Thomas, E.C., Villain, J.P., Cerisier, J.C., Senior, C., Hanuise, C., Hunsucker, R.D., Sofko, G., Koehler, J., Nielson, E., Pellinen, R., Walker, A. D. M., Sato, N. and Yamagishi, H. (1995): DARN/SuperDARN: A global view of the dynamics of high-latitude convection. *Space Sci. Rev.*, **71**, 761–793.
- Mendenhall, W., Scheaffer, R.L. and Wackerly, D.D. (1986): *Mathematical Statistics with Applications*. Boston, Duxbury Press.
- Palo, S.E., Portnyagin, Yu.I., Forbes, J.M., Makarov, N.A. and Merzlyakov, E.G. (1998): Transient eastward-propagating long-period waves observed over South Pole. *Ann. Geophys.*, **16**, 1486–1500.
- Portnyagin, Yu.I., Forbes, J.M. and Makarov, N.A. (1997): Unusual characteristics of lower thermosphere prevailing winds at South Pole. *Geophys. Res. Lett.*, **24**, 81–84.
- Portnyagin, Yu.I., Forbes, J.M., Makarov, N.A., Merzlyakov, E.G. and Palo, S. (1998): The summertime 12-hour wind oscillation with zonal wavenumber  $s=1$  in the lower thermosphere over South Pole. *Ann. Geophys.*, **16**, 828–837.
- Portnyagin, Yu.I., Forbes, J.M., Merzlyakov, E.G., Makarov, N.A. and Palo, S.E. (2000): Intradiurnal wind observations observed in the lower thermosphere over the South Pole. *Ann. Geophys.*, **18**, 547–554.
- Prikryl, P., Koehler, J.A. and Sofko, G.J. (1986): Simultaneous CW radio measurements of meteor and auroral drifts. *Radio Sci.*, **21**, 271–282.
- Reid, G.C. (1983): The influence of electric fields on radar measurements of winds in the upper mesosphere. *Radio Sci.*, **18**, 1028–1034.
- Ruohoniemi, J.M., Greenwald, R.A., Baker, K.B., Villain, J.-P., Hanuise, C. and McCready, M.A. (1987): Drift motions of small-scale irregularities in the high-latitude *F*-region - an experimental comparison with plasma drift motions. *J. Geophys. Res.*, **92**, 4553–4564.

*(Received December 12, 2000; Revised manuscript accepted May 15, 2001)*